



Intrinsic expression of viperin regulates thermogenesis in adipose tissues

John Eom^{a,1}, Jeong Jin Kim^{a,1}, Seul Gi Yoon^b, Haengdueng Jeong^a, Soojin Son^b, Jae Bong Lee^a, Jihye Yoo^a, Hyun Ju Seo^b, Yejin Cho^a, Ku Sul Kim^a, Kyung Mi Choi^a, Il Yong Kim^b, Hui-Young Lee^{c,d}, Ki Taek Nam^a, Peter Cresswell^{e,2}, Je Kyung Seong^{b,f,g,2}, and Jun-Young Seo^{a,2}

^aSeverance Biomedical Science Institute, Brain Korea 21 PLUS Project for Medical Science, Yonsei University College of Medicine, 03722 Seoul, Republic of Korea; ^bKorea Mouse Phenotyping Center, Seoul National University, 08826 Seoul, Republic of Korea; ^cDepartment of Molecular Medicine, School of Medicine, Gachon University, 21999 Incheon, Republic of Korea; ^dLee Gil Ya Cancer and Diabetes Institute, Gachon University, 21999 Incheon, Republic of Korea; ^eDepartment of Immunobiology, Yale University School of Medicine, New Haven, CT 06520; ^fLaboratory of Developmental Biology and Genomics, BK21 Program Plus for Advanced Veterinary Science, Research Institute for Veterinary Science, College of Veterinary Medicine, Seoul National University, 08826 Seoul, Republic of Korea; and ^gInterdisciplinary Program for Bioinformatics, Program for Cancer Biology, BIO-MAX/N-Bio Institute, Seoul National University, 08826 Seoul, Republic of Korea

Contributed by Peter Cresswell, June 25, 2019 (sent for review March 15, 2019; reviewed by Sheila Collins and Juan J. Lafaille)

Viperin is an interferon (IFN)-inducible multifunctional protein. Recent evidence from high-throughput analyses indicates that most IFN-inducible proteins, including viperin, are intrinsically expressed in specific tissues; however, the respective intrinsic functions are unknown. Here we show that the intrinsic expression of viperin regulates adipose tissue thermogenesis, which is known to counter metabolic disease and contribute to the febrile response to pathogen invasion. Viperin knockout mice exhibit increased heat production, resulting in a reduction of fat mass, improvement of high-fat diet (HFD)-induced glucose tolerance, and enhancement of cold tolerance. These thermogenic phenotypes are attributed to an adipocyte-autonomous mechanism that regulates fatty acid β -oxidation. Under an HFD, viperin expression is increased, and its function is enhanced. Our findings reveal the intrinsic function of viperin as a novel mechanism regulating thermogenesis in adipose tissues, suggesting that viperin represents a molecular target for thermoregulation in clinical contexts.

metabolism | fatty acid β -oxidation | innate immunity | viperin | thermogenesis

Many interferon (IFN)-inducible proteins play roles in defense against viral infection (1, 2). The mechanisms underlying the induction of these proteins are well established (3). Recently, technological advances in high-throughput analyses, such as RNA sequencing and proteomics, have enabled the generation of gene or protein expression profiles in various tissues. Unexpectedly, most IFN-inducible proteins, including Mx proteins (MX dynamin-like GTPases), GBPs (guanylate-binding proteins), ISG15 (IFN-stimulated gene product of 15 kDa), ISG20 (IFN-stimulated exonuclease of 20 kDa), IFITs (IFN-induced proteins with tetratricopeptide repeats), IFITMs (IFN-induced transmembrane proteins), BST2 (bone marrow stromal cell antigen 2), and viperin (virus-inhibitory protein, endoplasmic reticulum-associated, IFN-inducible), are expressed without any stimulation in certain tissues (4–7), suggesting that they may have novel and unexpected functions in such tissues.

Viperin (also known as RSAD2, cig5, or vig1) is an IFN-inducible multifunctional protein (8) that exhibits antiviral properties (9–12), mediates signaling pathways or Th2 cell development (13, 14), and regulates cellular metabolism (15, 16). The mechanisms by which viperin plays multiple roles in various cell types are well known. Viperin blocks the transport of soluble proteins from the endoplasmic reticulum to the Golgi apparatus (17). It also inhibits fatty acid β -oxidation in mitochondria, which in turn reduces ATP generation and enhances cellular lipogenesis (15, 16).

Adipose tissue is a central metabolic organ in the regulation of energy balance and homeostasis (18). There are 2 main types of adipose tissue: white adipose tissue (WAT) and brown adipose tissue (BAT). WAT functions to store fat, and BAT functions

mainly to burn fat for thermogenesis (19, 20). BAT has multiple mitochondria and multilocular lipid droplets, which are critical for heat generation by the induction of mitochondrial uncoupling protein 1 (UCP1) (21). WAT can also contribute to heat generation by a process known as browning, where it takes on characteristics of BAT (22–24). Activation of thermogenesis increases energy expenditure and improves metabolic complications such as obesity, insulin resistance, and type 2 diabetes (25–27). Induction of thermogenesis also requires adipose fatty acid β -oxidation (28–32). Similar to the phenotype of UCP1-deficient mice, the loss of adipose fatty acid β -oxidation in mice alters adiposity and causes sensitivity to cold (31, 32), suggesting that fatty acid β -oxidation is implicated in the control of thermogenesis and adipose tissue differentiation. However, it is not clear how fatty acid β -oxidation-mediated thermogenesis and differentiation are regulated.

Here we show that the intrinsic expression of viperin regulates thermogenesis in adipose tissues by inhibiting fatty acid β -oxidation. Viperin is naturally expressed in the adipose tissues of both specific

Significance

The expression of numerous interferon (IFN)-inducible proteins is triggered by IFN or stimuli that activate IFN signaling pathways in innate immune responses. However, many of these proteins are expressed without stimulation in specific tissues, suggesting that their intrinsic expression may have novel functions. We show here that viperin, an IFN-inducible protein, regulates fatty acid β -oxidation-mediated thermogenesis in adipose tissues. Viperin deficiency up-regulates the expression of thermogenesis- and fatty acid β -oxidation-related genes, which in turn increases heat production, reduces fat mass, improves high-fat diet-induced glucose tolerance, and enhances cold tolerance. Thus, the intrinsic expression of viperin plays a novel, pivotal role in thermoregulation.

Author contributions: P.C. and J.-Y.S. initiated research; J.K.S. and J.-Y.S. designed research; J.E., J.J.K., S.G.Y., H.J., and S.S. performed research; J.B.L., J.Y., H.J.S., Y.C., K.S.K., K.M.C., I.Y.K., H.-Y.L., and K.T.N. contributed new reagents/analytic tools; J.E., J.J.K., J.K.S., and J.-Y.S. analyzed data; and J.E., P.C., and J.-Y.S. wrote the paper.

Reviewers: S.C., Vanderbilt University Medical Center; and J.J.L., New York University School of Medicine.

The authors declare no conflict of interest.

Published under the PNAS license.

See Commentary on page 17145.

¹J.E. and J.J.K. contributed equally to this work.

²To whom correspondence may be addressed. Email: peter.cresswell@yale.edu, snumouse@snu.ac.kr, or jyseo0724@yuhs.ac.

This article contains supporting information online at www.pnas.org/lookup/suppl/doi:10.1073/pnas.1904480116/-DCSupplemental.

Published online July 24, 2019.

pathogen-free (SPF) and germ-free (GF) mice. We show that viperin deficiency reduces fat mass, increases lean body mass, improves high-fat diet (HFD)-induced glucose tolerance, and increases heat production. Viperin deficiency also up-regulates the expression of thermogenesis- and fatty acid β -oxidation-related genes in adipose tissues. Furthermore, cold exposure and a β -adrenergic receptor (ADRB3)-agonist promotes thermogenic phenotypes in viperin knockout (KO) mice. Finally, viperin regulates fatty acid β -oxidation-mediated thermogenesis in an adipocyte-autonomous manner. The expression of thermogenic genes is reduced only in viperin-deficient adipocytes after treatment with an inhibitor of fatty acid β -oxidation, etomoxir or ranolazine. Our data indicate that the natural expression of the IFN-inducible protein viperin plays a critical role in adipose tissue thermogenesis, and that viperin might be a molecular target for the activation of thermogenesis in metabolic disease prevention.

Results

Intrinsic Expression of Viperin Regulates Fat Metabolism and Heat Production. We hypothesized that intrinsic expression of the IFN-inducible protein viperin might provide a novel function in specific tissues. In this regard, we initially screened viperin expression in various tissues of SPF mice and GF mice (Fig. 1A). Viperin was expressed in the liver, heart, epididymal WAT (eWAT), inguinal WAT (iWAT), and BAT, but not in the brain. A comparison of tissue sizes in wild-type (WT) and viperin KO mice revealed larger eWAT and iWAT in the WT mice compared with the viperin KO mice (Fig. 1B). These results suggest that the intrinsic expression of viperin in adipose tissues could be involved in a regulatory function in metabolism. Increased expression of this protein in response to certain stimuli augments its intrinsic function, putatively leading to obesity.

To test this hypothesis, WT and viperin KO mice were fed either regular chow (RC) or an HFD from age 15 wk to 30 wk (15 wk on the diets; long period) (Fig. 1C). Unexpectedly, there was a slight difference in body weight between WT and viperin KO mice fed RC, but not between those fed an HFD (Fig. 1C). However, according to body composition analysis, the fat mass was decreased in viperin KO mice fed RC or an HFD (Fig. 1D). Except for the weight of adipose tissues, there was little difference in the weight of other tissues, spleen, kidney, and testis between WT and viperin KO mice (*SI Appendix, Fig. S1A*). This suggests that viperin exerts tissue-specific effects. Viperin expression was increased in the adipose tissues of WT mice after feeding an HFD (Fig. 1E). Therefore, viperin deficiency reduced the size of adipocytes (Fig. 1F and *SI Appendix, Fig. S1B*). In addition, it resulted in a decrease in the size of hepatic lipid droplets that accumulated in HFD-fed mice (Fig. 1F and *SI Appendix, Fig. S1B*). Viperin deficiency also reduced total cholesterol levels in serum of mice fed RC or an HFD, decreased aspartate aminotransferase (AST) and alanine aminotransferase (ALT) levels in serum of mice fed an HFD, and improved HFD-induced glucose tolerance (Fig. 1G and H).

We analyzed the metabolic phenotypes of WT and viperin KO mice by performing indirect calorimetry (Fig. 1I and *SI Appendix, Fig. S1C*). Interestingly, viperin deficiency significantly increased the rates of heat production, oxygen consumption, and carbon dioxide production. Given that adipose fatty acid β -oxidation is required for thermogenesis (28–32), this finding suggests a possible role for viperin in thermogenesis in adipose tissues. Moreover, the high rate of food intake in viperin KO mice suggested that their decreased fat phenotype was possibly caused by active thermogenesis.

We also compared the phenotypes of WT and viperin KO mice fed RC or an HFD at different ages and periods. Mice were fed RC or an HFD from age 6 wk to 21 wk (15 wk on the diets) (*SI Appendix, Fig. S2*) or from age 16 wk to 20 wk (4 wk on the diets; short period) (*SI Appendix, Fig. S3*). The phenotype

comparisons were repeated in all mice, except those fed an HFD for a short period (*SI Appendix, Fig. S2 A–F and S3 A–E*). The results indicate that viperin-mediated phenotypes are dependent on duration of the feeding period rather than on the age of mice.

Viperin Deficiency Promotes Thermogenic Gene Expression in Adipose Tissues. To determine whether viperin expression is involved in fatty acid β -oxidation-mediated thermogenesis, we measured the expression levels of canonical thermogenesis-related genes, such as *Ucp1*, *Pgc1 α* , and *Cidea*, and fatty acid β -oxidation-related genes, such as *Ppara*, *Ppar β/δ* , and *Cpt1*, in adipose tissues (Fig. 2A and *SI Appendix, Figs. S4 and S5*). The expression levels of these genes were significantly increased in adipose tissues, especially the eWAT and iWAT of viperin KO mice fed RC (Fig. 2A and *SI Appendix, Figs. S4A and S5A*). These genes were also significantly up-regulated in the iWAT and BAT of viperin KO mice fed an HFD for an extended period, but not in those fed an HFD for a short period (Fig. 2A and *SI Appendix, Figs. S4B and S5B*). UCP1 protein expression was increased in the adipose tissues of viperin KO mice fed RC or an HFD (Fig. 2B and C). Viperin expression was increased in the adipose tissues of WT mice fed an HFD (Fig. 2B and *SI Appendix, Fig. S6A*). Moreover, viperin localized to the mitochondria in the BAT of WT mice fed RC or an HFD (Fig. 2D). The data indicate that viperin down-regulates thermogenesis in adipose tissues, possibly by inhibiting fatty acid β -oxidation in the mitochondria of adipocytes. Cytokines, including IL-10 and IL-13, from immune cells such as macrophages and eosinophils reportedly regulate thermogenesis in adipose tissues (33–35). We recently showed that viperin deficiency promotes the secretion of proinflammatory and anti-inflammatory cytokines from completely differentiated bone marrow-derived macrophages (36). However, viperin was not detected in macrophages in the BAT of mice fed RC. We observed only a small number of viperin-expressing macrophages in the BAT of mice fed an HFD, although the number of macrophages infiltrating the BAT increased after feeding an HFD (*SI Appendix, Fig. S6B*). Except for the BAT of mice fed RC, there was little difference in the expression levels of cytokine genes in adipose tissues between WT and viperin KO mice fed RC or an HFD (*SI Appendix, Fig. S6 C and D*).

Viperin Deficiency Enhances Thermogenesis and Leads to Cold Tolerance. To confirm the requirement of viperin for the regulation of thermogenesis in adipose tissues, we kept WT and viperin KO mice fed RC at 4 °C for 7 d and measured their core body temperature at different time intervals. Body temperature was higher in viperin KO mice compared with WT mice during chronic cold exposure for 7 d (Fig. 3A), indicating that viperin deficiency promotes cold tolerance. Adipose tissue mass decreased in viperin KO mice exposed to cold (Fig. 3B), suggesting that thermogenesis is more active in viperin KO mice than in WT mice during cold exposure. The expression of thermogenesis- and fatty acid β -oxidation-related genes was highly elevated in the adipose tissues of viperin KO mice exposed to cold (Fig. 3C). Viperin protein expression was increased in the BAT of WT mice after cold exposure (Fig. 3D); however, the increases in expression levels of UCP1 protein in the BAT and the adipocytes were greater in viperin KO mice compared with WT mice exposed to cold (Fig. 3D and E). The data indicate that the increases in viperin expression enhance its inhibitory function in thermogenesis under cold conditions and thus reduce cold tolerance. Therefore, viperin is required for the regulation of cold-induced thermogenesis in adipose tissues.

Viperin Deficiency Facilitates Cold-Induced Thermogenesis via the Adrenergic Signaling Pathway. Next, to determine whether the phenotype of cold-induced thermogenesis in the adipose tissues of viperin KO mice is mediated by the adrenergic signaling

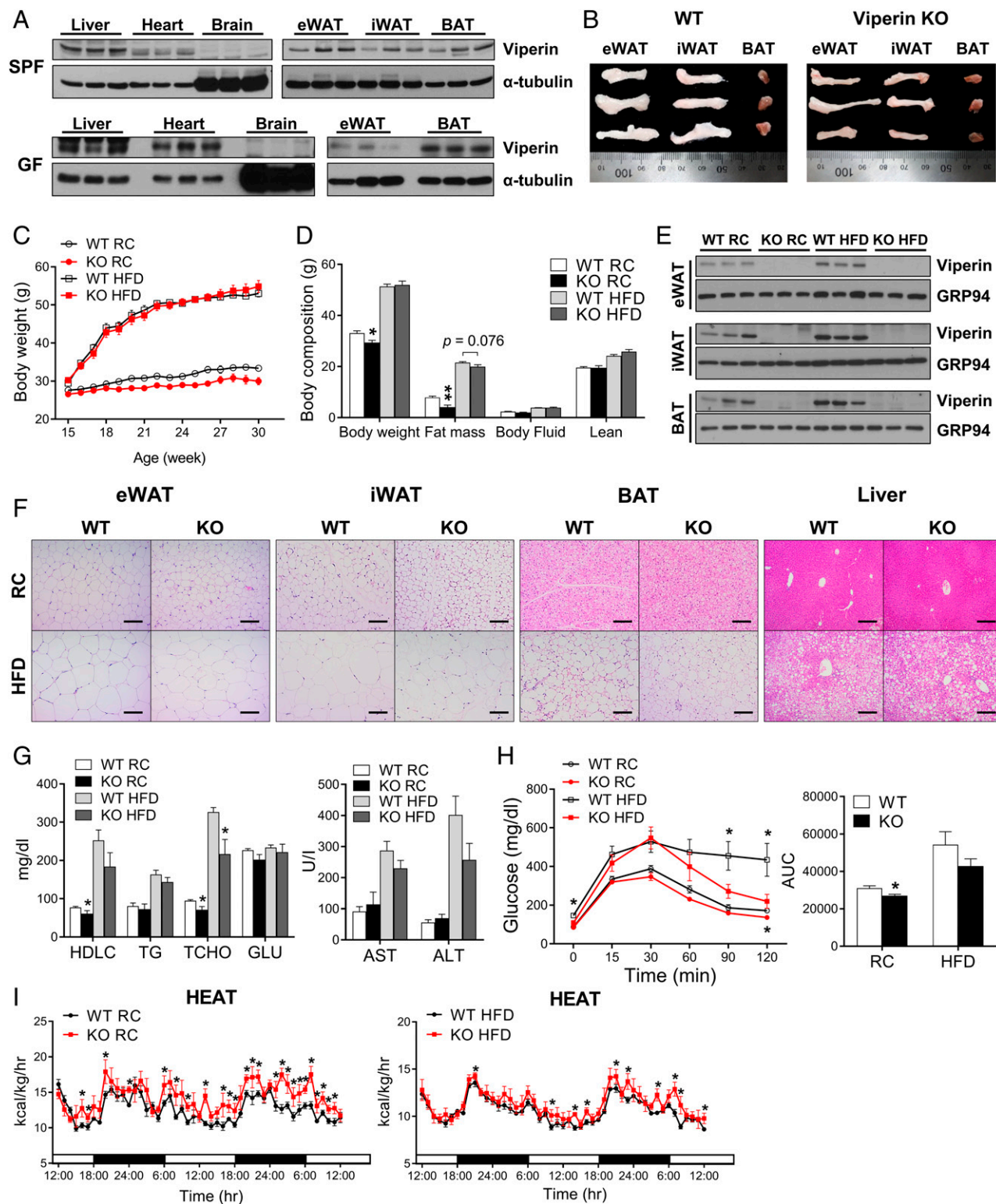


Fig. 1. Intrinsic expression of viperin in adipose tissues regulates fat metabolism and heat production. (A) Expression of viperin in various tissues of SPF and GF mice. (B) Gross morphology of the adipose tissues eWAT, iWAT, and BAT of WT and viperin KO mice. (C–I) WT and viperin KO mice were fed RC or an HFD from age 15 wk to 30 wk (15 wk on diet). Body weight ($n = 4-7$) (C); body composition ($n = 4-7$) (D); expression of viperin in adipose tissues ($n = 3$) (E); representative H&E-stained sections from adipose tissues and liver (Scale bar: 200 μm) (F); serum metabolites (HDLC, TG, TCHO, and GLU), AST, and ALT ($n = 4-7$) (G); i.p. glucose tolerance test, including area under the curve ($n = 7-8$) (H); and heat production rates ($n = 4-7$; indirect calorimetry) (I) of WT and viperin KO mice fed RC or an HFD. Data are presented as mean \pm SEM of biologically independent samples. * $P < 0.05$; ** $P < 0.01$; *** $P < 0.001$ vs. WT on the same diet.

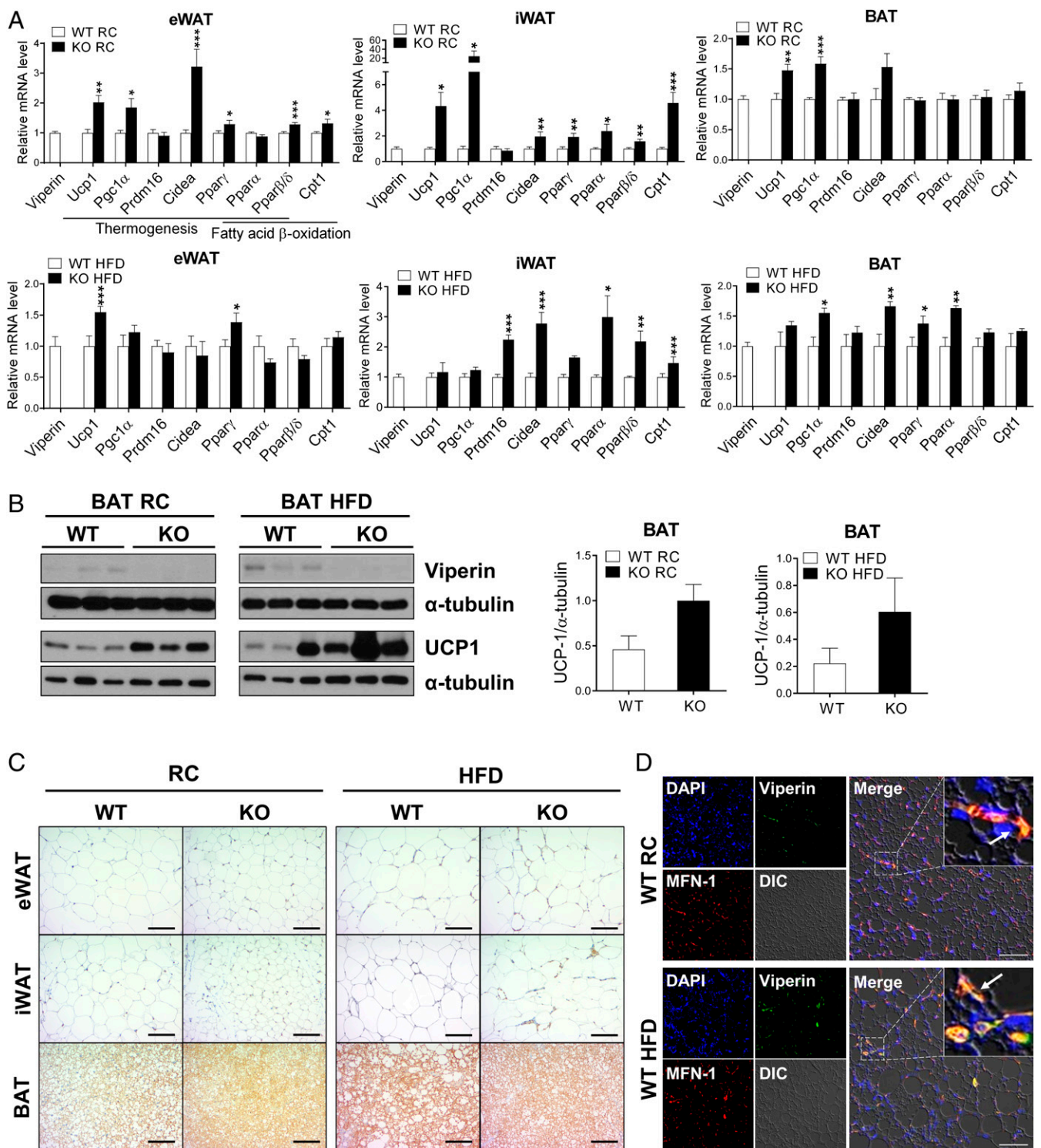


Fig. 2. Viperin deficiency promotes expression of thermogenesis-related genes and proteins in adipose tissues. The adipose tissues are isolated from WT and viperin KO mice fed RC or an HFD for 15 wk. (A) Relative mRNA levels of thermogenesis- and fatty acid β -oxidation-related genes in adipose tissues ($n = 6$). (B) Protein expression of viperin and UCP1 in BAT ($n = 3$). (C) Immunohistochemical staining for UCP1 in adipose tissues. (Scale bar: 200 μ m.) (D) Immunofluorescence staining of adipose tissues. DAPI, nucleus (blue); viperin (green); MFN-1, a mitochondrial marker (red). Arrows indicate viperin localized to the mitochondria. (Scale bar: 50 μ m.) Data are presented as mean \pm SEM of biologically independent samples. * $P < 0.05$; ** $P < 0.01$; *** $P < 0.001$ vs. WT on the same diet.

pathway, mice were stimulated with the ADRB3 agonist CL-316243 for 3 d. Indirect calorimetry showed that the rates of heat production, oxygen consumption, and CO_2 production were significantly increased in CL-treated viperin KO mice (Fig. 4A

and *SI Appendix, Fig. S7*). However, there was no difference in the rate of food intake between CL-treated WT and viperin KO mice (*SI Appendix, Fig. S7*). These results indicate that viperin regulates thermogenesis in adipose tissues independent of food

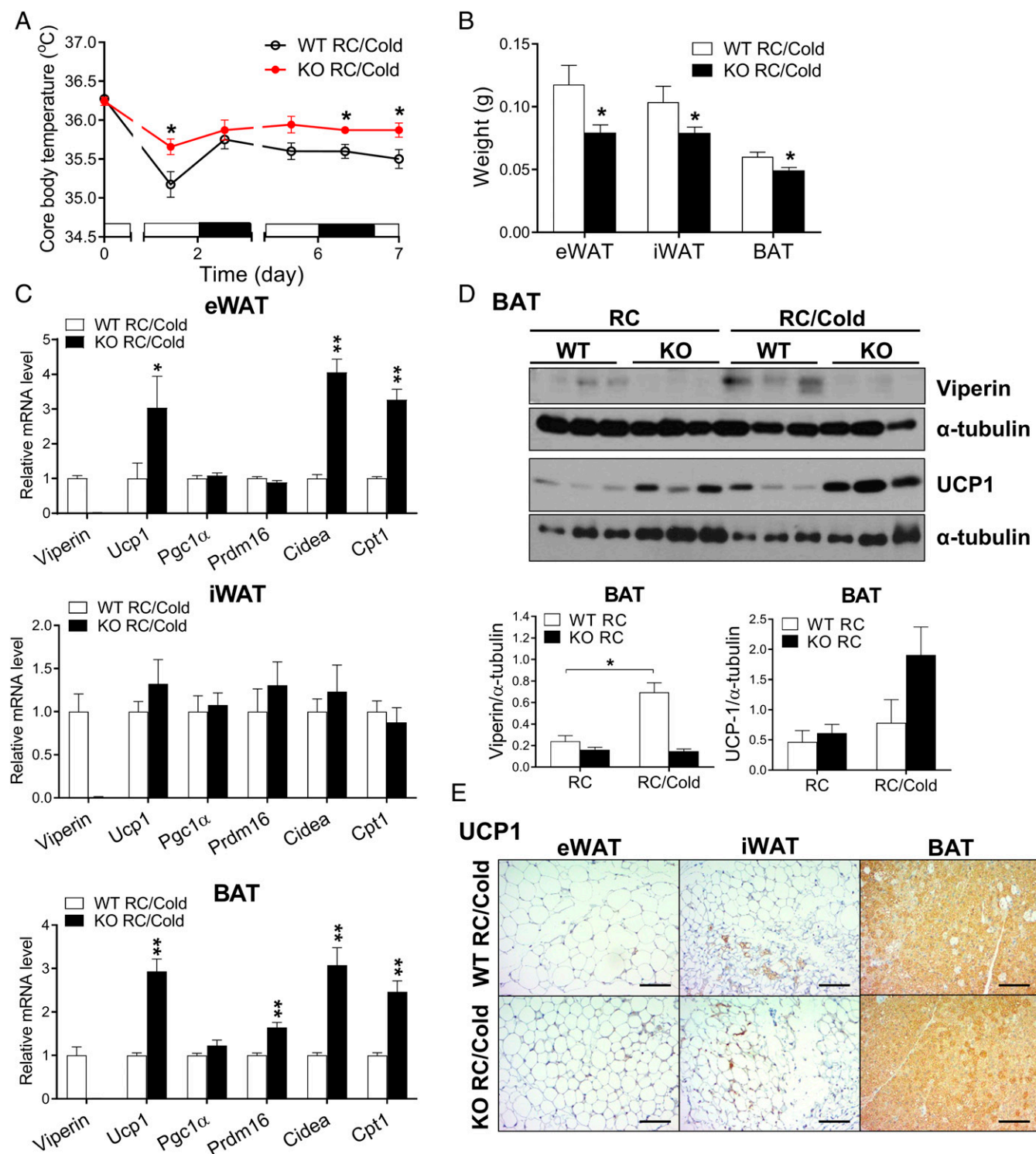


Fig. 3. Viperin deficiency enhances thermogenesis and leads to cold tolerance. (A) Rectal temperature of 21-wk-old WT and viperin KO mice during chronic cold exposure for 7 d ($n = 4-7$). (B-E) Gross weights of adipose tissues ($n = 4-7$) (B), relative mRNA levels of thermogenesis- and fatty acid β -oxidation-related genes in adipose tissues ($n = 4-7$) (C), protein expression of viperin and UCP1 in the BAT ($n = 3$) (D), and immunohistochemical staining for UCP1 in adipose tissues (Scale bar: 200 μ m) (E) of WT and viperin KO mice after chronic cold exposure.

intake. Glucose tolerance was improved, and the adipose tissue mass was reduced in CL-treated viperin KO mice (Fig. 4B and C), suggesting that thermogenesis is highly active in CL-treated viperin KO mice. The expression levels of thermogenesis- and fatty acid β -oxidation-related genes were highly elevated in the

adipose tissues of CL-treated viperin KO mice (Fig. 4D). Viperin protein expression was increased in the iWAT of CL-treated WT mice (Fig. 4E). Like in mice exposed to cold, the increases in expression levels of UCP1 protein in adipose tissues were greater in CL-treated viperin KO mice compared with CL-treated WT

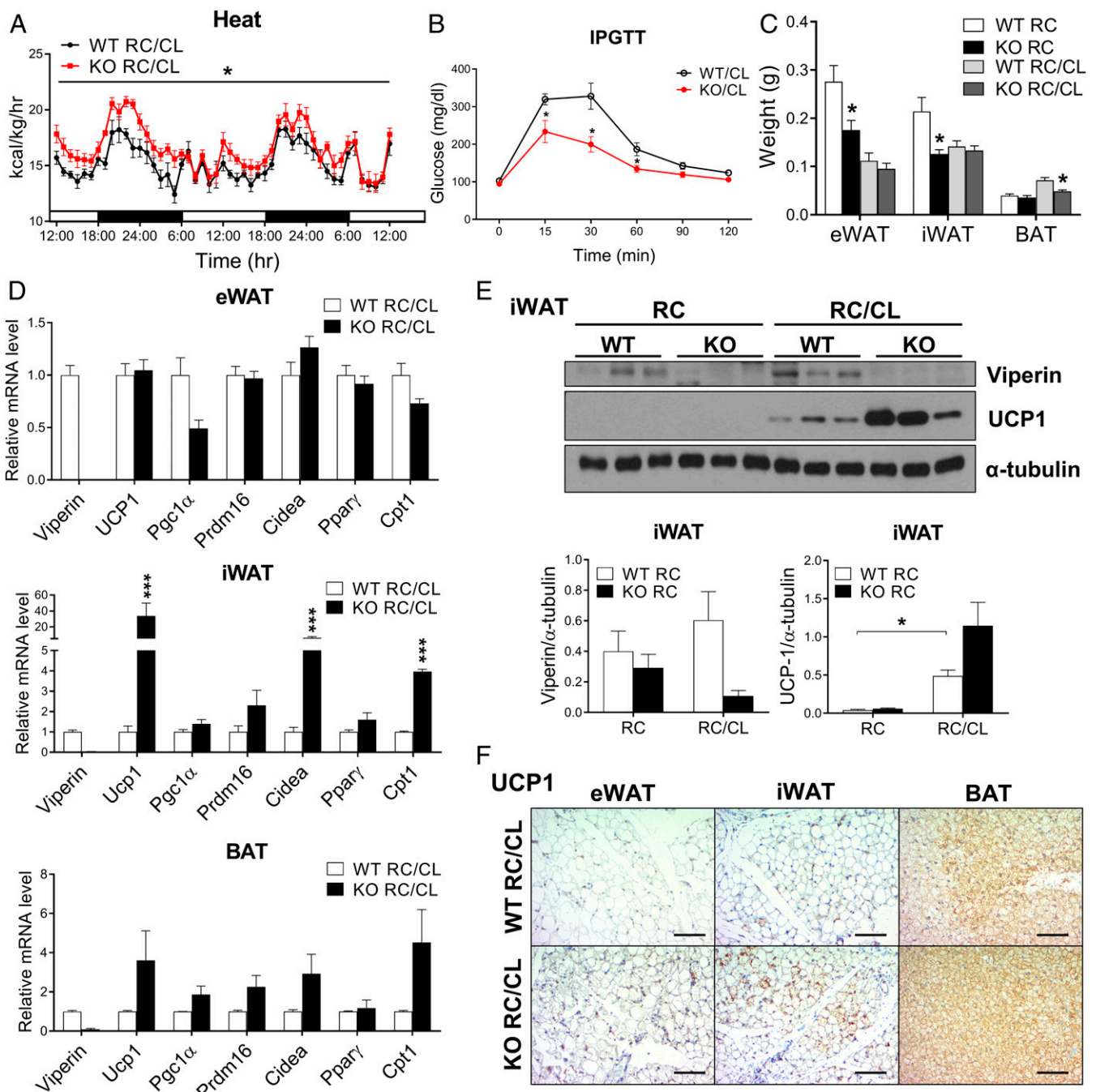


Fig. 4. The ADRB3 agonist promotes thermogenic phenotypes in viperin KO mice. WT and viperin KO mice were administered i.p. with CL-316243, an ADRB3 agonist (1 mg/kg body weight/d) for 3 d. (A–F) Heat production rates ($n = 6$; indirect calorimetry) (A), i.p. glucose tolerance test ($n = 6$) (B), gross weight of adipose tissues ($n = 6$) (C), relative mRNA levels of thermogenesis- and fatty acid β -oxidation-related genes in the adipose tissues ($n = 6$) (D), protein expression levels of viperin and UCP1 in iWAT ($n = 3$) (E), and immunohistochemical staining for UCP1 in adipose tissues (Scale bar: 200 μ m) (F) of CL-treated mice. Data are represented as mean \pm SEM of biologically independent samples. * $P < 0.05$; ** $P < 0.001$ vs. WT for the same treatment.

mice (Fig. 4 E and F). These findings indicate that the cold-induced phenotype of viperin KO mice is mediated by the adrenergic signaling pathway.

HFD-Induced Viperin Expression Augments the Phenotypes of Cold-Induced Thermogenesis. Since viperin expression was increased in the adipose tissues of WT mice after feeding an HFD or cold exposure, we monitored thermogenic phenotypes of WT and viperin KO mice fed an HFD after cold exposure or CL treatment. Mice were fed HFD at 4 $^{\circ}$ C for 7 d and measured their

core body temperature at different time intervals (SI Appendix, Fig. S8 A–C). Similar to the results from mice fed RC after cold exposure, body temperature was higher in viperin KO mice fed an HFD compared with WT mice during chronic cold exposure for 7 d (SI Appendix, Fig. S8A). Viperin expression was highly increased in the BAT of WT mice fed an HFD after cold exposure (SI Appendix, Figs. S8B and S9). The increased UCP1 expression levels in the BAT and the adipocytes were more significant in viperin KO mice fed an HFD compared with WT mice fed an HFD exposed to cold (SI Appendix, Fig. S8 B and C). The findings

indicate that HFD- and cold-induced viperin expression amplifies its inhibitory function in thermogenesis and augments the thermogenic phenotypes of WT and viperin KO mice. We also determined whether the phenotype of cold-induced thermogenesis in the adipose tissues of viperin KO mice fed an HFD is mediated by the adrenergic signaling pathway. Mice fed an HFD were stimulated with the ADRB3 agonist CL-316243 for 3 d (*SI Appendix, Fig. S8 D–G*). HFD-induced glucose tolerance was improved, suggesting that thermogenesis is highly active in CL-treated viperin KO mice fed an HFD (*SI Appendix, Fig. S8D*). Viperin protein expression was increased in the iWAT and BAT of CL-treated WT mice fed an HFD (*SI Appendix, Fig. S8 E and F*). The increases in UCP1 expression levels in the adipose tissues were greater in CL-treated viperin KO mice fed an HFD compared with CL-treated WT mice fed an HFD (*SI Appendix, Fig. S8 E–G*). These findings indicate that the cold-induced phenotype of viperin KO mice fed an HFD is mediated by the adrenergic signaling pathway. Taken together, our data demonstrate that viperin is required for the regulation of thermogenesis in adipose tissues, and that its function is accelerated under an HFD and/or cold conditions.

Viperin Regulates Fatty Acid β -Oxidation–Mediated Thermogenesis in an Adipocyte-Autonomous Manner. To test the cell-autonomous function of viperin in adipose tissues, the stromal vascular fraction (SVF) was isolated from BAT or eWAT and differentiated into mature brown or white adipocytes (Fig. 5 and *SI Appendix, Figs. S10 and S11*). Viperin deficiency was found to enhance the expression of adipogenesis-related genes, such as *Adiponectin*, *Fabp4*, and *C/ebp α* , and thermogenesis- and fatty acid β -oxidation-related genes in mature brown adipocytes (Fig. 5A and *SI Appendix, Fig. S10A*) and mature white adipocytes (*SI Appendix, Fig. S11A*). This finding suggests that the up-regulation of fatty acid β -oxidation facilitates both adipogenesis and thermogenesis in adipocytes.

To exclude the possibility that cytokines from immune cells in adipose tissues affect the thermogenic phenotypes in the adipocytes, we measured the expression levels of cytokines in the SVF isolated from BAT of the WT and viperin KO mice as well as in the SVF-differentiated brown adipocytes (*SI Appendix, Fig. S10B*). Since SVF contains immune cells as well as preadipocytes, the cytokines are likely to be derived from the immune cells in the culture. There was little difference in cytokine expression between WT and viperin KO SVF or adipocytes. These data indicate that viperin regulates thermogenesis in an adipocyte-autonomous manner. The increase in thermogenesis-related gene expression in response to CL treatment was significantly augmented in viperin KO brown adipocytes, since viperin expression was increased in the WT brown adipocytes in response to CL treatment (Fig. 5B). This finding indicates that viperin inhibits thermogenic activity in the BAT.

Finally, to identify the potential mechanism by which viperin regulates thermogenesis in adipose tissues, we measured the expression levels of the thermogenesis-related genes in adipocytes treated with an inhibitor of fatty acid β -oxidation, either etomoxir or ranolazine (Fig. 5C and *SI Appendix, Fig. S11B*). The expression of thermogenesis-related genes was significantly reduced only in viperin KO adipocytes after inhibitor treatment. These observations indicate that viperin deficiency induces the up-regulation of thermogenesis by facilitating fatty acid β -oxidation in adipocytes.

Analysis of extracellular flux showed an increased oxygen consumption rate (OCR) in viperin KO brown adipocytes. Mitochondrial parameters, including basal respiration, ATP production, proton leak, and maximal respiration, were also calculated from the OCR before and after the addition of mitochondrial respiratory chain inhibitors. Proton leak (uncoupled respiration), a key component of thermogenesis, and the other parameters were

increased in viperin KO brown adipocytes. Moreover, the increase in proton leak in response to CL treatment was augmented in viperin KO brown adipocytes (Fig. 5D). Conversely, the proton leak was reduced only in viperin KO brown adipocytes after etomoxir treatment (Fig. 5D). Our data indicate that viperin expression inhibits fatty acid β -oxidation and thus negatively regulates adipogenesis and thermogenesis in adipocytes.

Discussion

Viperin is induced in various cell types by IFNs (types I, II, and III), double-stranded (ds) B-form DNA, dsRNA, poly I:C, lipopolysaccharides, and infection with many viruses (8). Here we identified the intrinsic expression of viperin without any stimulation in specific tissues. Our data identify the intrinsically expressed viperin as a pivotal regulator of thermogenesis in adipose tissues. Furthermore, in response to certain stimuli, viperin expression is increased, and its intrinsic function is exaggerated.

The 3 types of adipose tissue—eWAT, iWAT, and BAT—differ at the phenotype level between WT and viperin KO mice. Viperin deficiency reduces the size of adipocytes in these adipose tissues. Notably, eWAT and iWAT of viperin KO mice are smaller and have a reddish-brown tint. Moreover, viperin deficiency elevates the expression of thermogenesis- and fatty acid β -oxidation-related genes in eWAT, iWAT, and BAT. Given that WAT contributes to browning and thermogenesis and develops BAT-like characteristics (22–24), our data suggest that viperin deficiency may increase browning of WAT. In addition, viperin deficiency decreases the size of hepatic lipid droplets accumulating in the liver and the levels of AST and ALT in serum of mice fed an HFD. These findings suggest that viperin deficiency may reduce hepatic steatosis in HFD-induced non-alcoholic fatty liver disease.

Viperin deficiency increases the rate of food intake. This observation suggests that viperin may regulate the production of orexigenic factors, such as neuropeptide Y, in the brain (37, 38). Its possible role in the brain needs further elucidation. Despite a high rate of food intake, the fat mass is decreased in viperin KO mice. The rates of activity and fecal energy loss do not differ between WT and viperin KO mice; however, the rate of heat production is significantly higher in viperin KO mice. The data suggest that viperin deficiency actively induces thermogenesis in adipose tissues and thus overcomes lipid accumulation from the high rate of food intake, resulting in a reduction of fat mass. Moreover, viperin deficiency activates thermogenesis in adipose tissues independent of food intake, as confirmed by the augmented thermogenic phenotype of viperin KO mice when exposed to cold or CL treatment, without differences in rates of food intake.

Diet- or cold-induced activation of adipose tissues, especially BAT, increases lipolysis and fatty acid β -oxidation, resulting in the generation of heat via UCP1 at the expense of stored lipids (39). Diet- or cold-induced activation of thermogenesis is a means of preventing obesity (40, 41). On HFD stimulation or exposure to cold, an increase in viperin expression has an inhibitory role in the activation of thermogenesis. There is no difference in the thermogenic phenotypes between WT and viperin KO mice fed an HFD for a short period, suggesting that the level of HFD-induced activation of thermogenesis is higher than that of viperin-mediated inhibition of thermogenesis for a short period. However, the difference in thermogenic phenotypes is augmented in mice fed an HFD for an extended period, since viperin expression is increased and the level of viperin-mediated inhibition of thermogenesis is elevated during this period. Similarly, the thermogenic phenotypes in WT and viperin KO mice exposed to cold could be explained by the levels of cold-induced viperin expression and viperin-mediated inhibition of thermogenesis. Cold exposure up-regulates the expression of thermogenesis- and fatty acid β -oxidation-related genes/proteins,

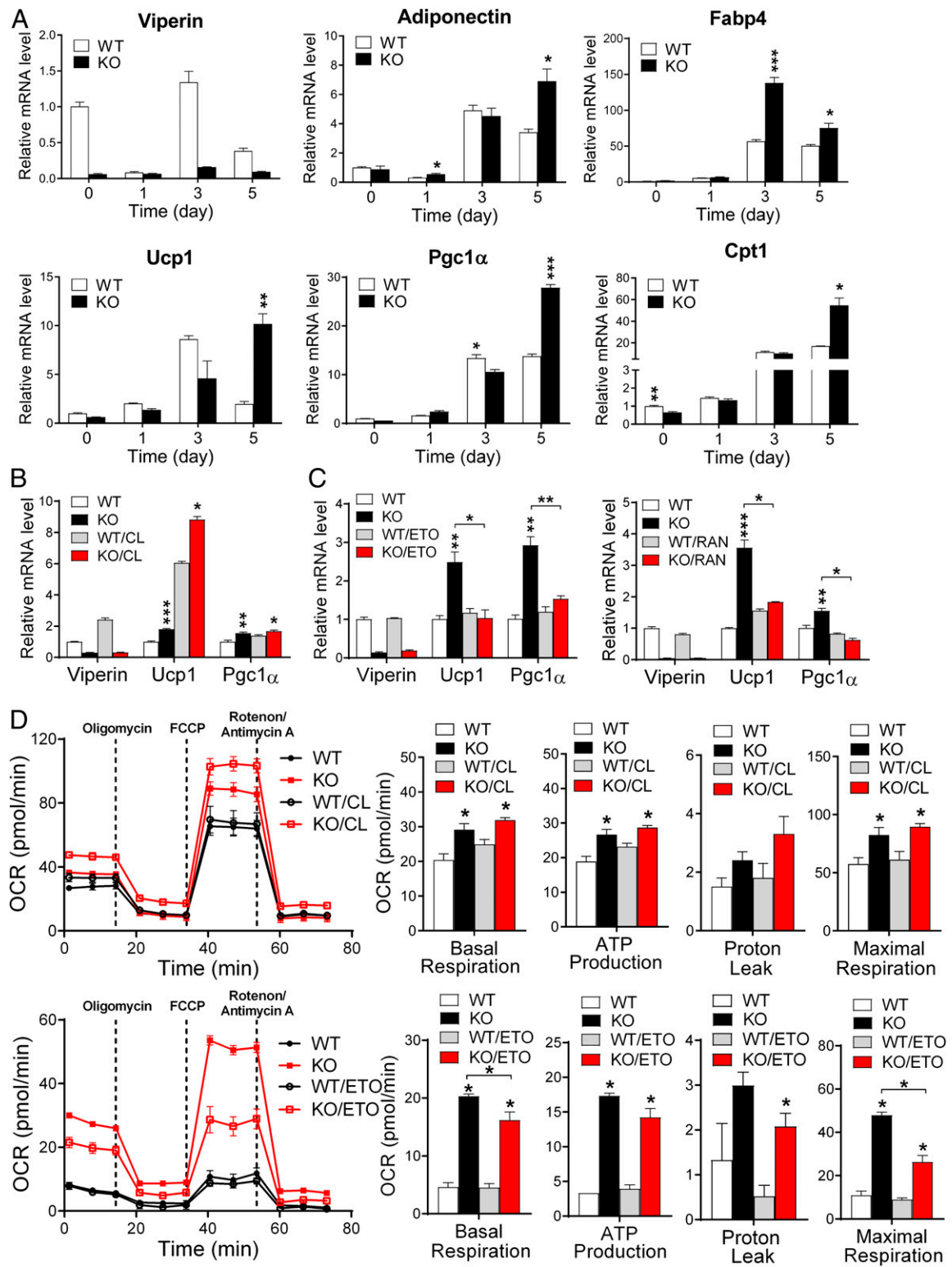


Fig. 5. Viperin regulates fatty acid β -oxidation-mediated thermogenesis in an adipocyte-autonomous manner. SVF is isolated from the BAT and differentiated into mature brown adipocytes. (A) Relative mRNA levels of adipogenesis-, thermogenesis-, and fatty acid β -oxidation-related genes in brown adipocytes during differentiation. (B and C) Relative mRNA levels of thermogenesis-related genes in CL-treated brown adipocytes (B) and etomoxir (ETO; Left)- or ranolazine (RAN; Right)-treated brown adipocytes (C). (D) OCR and mitochondrial parameters (basal respiration, ATP production, proton leak, and maximal respiration) in WT and viperin KO brown adipocytes after CL treatment (Top) or ETO treatment (Bottom). Data are presented as mean \pm SEM of 2 independent experiments. * $P < 0.05$; ** $P < 0.01$; *** $P < 0.001$ vs. WT for the same treatment.

resulting in active thermogenesis in both WT and viperin KO mice. However, cold-induced viperin suppresses the expression of these genes/proteins, and thus the increase in thermogenesis is lower in WT mice compared with viperin KO mice during cold exposure. This suggests that viperin may function as a brake on an uncontrolled increase in thermogenesis. Our results indicate that increased viperin expression in response to certain stimuli enhances its intrinsic function in adipose tissues.

Viperin is expressed in SVF-differentiated adipocytes. Viperin deficiency increases expression of adipogenesis-, thermogenesis-, and fatty acid β -oxidation-related genes in these adipocytes. Treatment with an inhibitor of fatty acid β -oxidation, either etomoxir or ranolazine, reduces thermogenic phenotypes only in viperin KO adipocytes. Moreover, viperin deficiency does not affect HFD-induced inflammation in adipose tissues. Therefore, our data show that viperin regulates fatty acid β -oxidation-mediated thermogenesis in an adipocyte-autonomous manner.

Adipose tissue thermogenesis also contributes to the heat production necessary to raise the core body temperature during the febrile response to pathogen invasion (42–45). In viral or bacterial infections, an increase in viperin expression may play an inhibitory role in the febrile response as a host defense mechanism. In contrast, increased viperin expression may also play a protective role in the lethal febrile response to pathogens that cause hemorrhagic fever, such as the Ebola, Marburg, Lassa fever, and yellow fever viruses. Given the importance of thermoregulation, our results demonstrate that the intrinsic expression of viperin in adipose tissues plays a role in homeostasis of body temperature in terms of the body's defense mechanisms. Since viperin expression is increased under certain circumstances that disrupt homeostasis, viperin represents a molecular target for the regulation of thermogenesis in clinical contexts. Overall, our results suggest that the intrinsic expression of IFN-inducible proteins may exert their own intrinsic functions in specific tissues.

Materials and Methods

Animal Procedures. All animal experiments were conducted in accordance with the guidelines of and approved by the Institutional Animal Care and Use Committee of Yonsei University Health System. Mice were maintained under a 12-h light/12-h dark cycle at 22 °C in a SPF barrier facility, with free access to water and chow.

Animals and Diets. The WT and viperin (*Rsd2*) KO C57BL/6 male mice were used in this study have been described previously (14). The WT and viperin KO mice were cohoused and fed RC or an HFD (i.e., 60% of the total calories from fat, 20% from carbohydrate, and 20% from protein) (D12492; Research Diets) from age 15 wk to 30 wk (15 wk on diet), from age 6 wk to 21 wk (15 wk on diet), or from age 16 wk to 20 wk (4 wk on diet).

Tissue Isolation. The liver, heart, midbrain, eWAT, iWAT, and BAT were collected from WT and viperin KO mice fed RC or an HFD. Tissues of GF C57BL/6 mice were kindly provided by Dr. Charles D. Surh (POSTECH).

Body Composition and Blood Chemistry Analysis. Fat and lean body mass values were assessed by ^1H magnetic resonance spectroscopy (Bruker). Serum was collected from all mice. High-density lipoprotein cholesterol (HDL), triglycerides (TG), total cholesterol (TCHO), glucose (GLU), AST, and ALT concentrations were measured calorimetrically using a Roche cobas c111 analyzer.

Glucose Tolerance Test. Mice were fasted for 16 h. Glucose (1 g/kg body weight) was administered i.p., and blood glucose levels were measured at 0, 15, 30, 45, 60, and 120 min with a glucometer (Allmedicus).

Indirect Calorimetry. Metabolic performance (energy intake and energy expenditure) was measured with an automated combined indirect calorimetry system (Phenomaster; TSE Systems). Before the experiment, the mice were acclimated for 2 d in a metabolic chamber with chow and water. Then oxygen consumption rate (VO_2 ; mL/kg/h), carbon dioxide production rate (VCO_2 ; mL/kg/h), heat production rate (energy expenditure; kcal/kg/h), food intake rate (kcal/kg/h), respiratory exchange ratio (RER; VCO_2/VO_2), and activity were measured for 3 d. Heat production and RER were calculated from the gas

exchange data. Activity was measured using infrared beams to count the beam breaks during an indicated measurement period. The metabolic data were normalized with respect to lean body weight. All mice were maintained under a 12-h light/12-h dark cycle at 22 °C.

Body Temperature and Cold Exposure. For thermoneutral adaptation, 20-wk-old WT and viperin KO male mice (1 mouse per cage) were cohoused in an animal incubator (Dae Han Bio Link) at 30 °C on a 12-h light/12-h dark cycle with access to RC or an HFD for 2–3 d (46, 47). For the cold challenge, the incubator was cooled to 4 °C, and the mice were kept in it with free access to water and chow for 7 d. Core body temperature was measured rectally at different time intervals during the cold challenge. In addition, the ADRB3 agonist CL-316243 (Sigma-Aldrich), 1 mg/kg body weight/d, was administered i.p. to 21-wk-old WT and viperin KO mice fed RC or an HFD for 3 d.

Histological Analysis. Adipose tissues were harvested, fixed in 4% (wt/vol) paraformaldehyde in PBS, and embedded in paraffin. The paraffin-embedded tissue sections were deparaffinized with xylene and rehydrated with 100%, 95%, and 70% (vol/vol) ethanol. These samples were used for hematoxylin and eosin (H&E) staining, immunohistochemistry, and immunofluorescence analyses. Antigens were retrieved in target retrieval solution in a pressure cooker (Dako Denmark). Endogenous peroxidase activity was blocked with 3% H_2O_2 (vol/vol) followed by protein blocking in a serum-free, ready-to-use protein block solution (Dako Denmark). For immunofluorescence, the samples were then treated with primary antibodies specific to viperin (MaP.VIP), MFN-1 (Santa Cruz Biotechnology), and UCP1 (Abcam) and secondary Alexa Fluor 488- or 555-conjugated antibodies (Invitrogen). Images were captured with a confocal microscope system (LSM 700; Carl Zeiss).

Quantitative Image Analysis. Representative images were captured under light microscopy (Olympus BX43). The size of adipocytes and hepatic lipid droplets was analyzed by Toup view 3.7. For quantitation, 5 fields were chosen at random for each sample, and the diameter of adipocytes and hepatic lipid droplets was measured in the optical field at 200 \times magnification. Mean diameter was calculated from the number of measured adipocytes and hepatic lipid droplets.

Immunoblot Analysis. Adipose tissues collected from WT and viperin KO mice were homogenized in 1 \times RIPA buffer with protease inhibitors (Complete Mini; F. Hoffmann-La Roche) and phosphatase inhibitors (PhosSTOP; F. Hoffmann-La Roche). All samples were centrifuged at 6,000 \times g for 20 min at 4 °C, and the supernatants were collected. Protein concentrations were measured by a bicinchoninic acid assay (Thermo Fisher Scientific). The proteins were separated by 10% SDS/PAGE gels and transferred to PVDF membranes. The blots were blocked in 5% skim milk and 0.05% Tween in PBS for 1 h, incubated with primary antibodies, probed with anti-Ig horseradish-conjugated secondary antibodies, and incubated with enhanced chemiluminescence reagents (Thermo Fisher Scientific). GRP94 (Abcam, Cambridge, UK) or α -tubulin was used as a loading control.

RNA Extraction, cDNA Preparation, and Quantitative Real-Time PCR. The Qiagen RNeasy Mini Kit was used to isolate total RNA from cells or adipose tissues. cDNA synthesis was performed with 1 μ g of RNA using the Prime Script First-Strand cDNA Synthesis Kit (TaKaRa Bio) according to the manufacturer's instructions. The cDNA was quantified by qRT-PCR using the SYBR Green PCR Kit (Applied Biosystems). The reaction was performed at 95 °C for 10 min, followed by a 3-step PCR program of 95 °C for 30 s, 55 °C for 1 min, and 72 °C for 30 s repeated for 50 cycles. The primers used in the PCR are listed in *SI Appendix, Table S1*. CPT1 has 3 different isoforms: CPT1A, CPT1B, and CPT1C. Primers for *Cpt1b* were used in this study. The PCR was performed in triplicate for each sample. Quantitation was performed by the comparative $2^{-\Delta\Delta\text{Ct}}$ method. The Ct value for each sample was normalized to that of the β actin gene. Two independent experiments were statistically analyzed for differences in their means, and the *P* values are indicated in the figures.

SVF Isolation and Differentiation to Adipocytes. Brown and white adipose SVFs were obtained from 3-to-6-wk-old male mice fed RC as described previously, with some modifications (48). In brief, adipose tissue was minced and digested for 50 min at 37 °C in Hanks' balanced salt solution containing 1 mg/mL type 1 collagenase (Worthington Biochemical). The tissue suspensions were filtered through a 45- μ m cell strainer and centrifuged at 470 \times g for 15 min to pellet the SVF. The pellet was resuspended in adipocyte culture medium supplemented with 10% FBS and 1% penicillin/streptomycin and

then plated. Once confluence was reached, the primary brown adipocytes were induced to differentiate with 500 μ M of 3-isobutyl-1-methylxanthine (IBMX), 0.5 μ M dexamethasone, 20 nM insulin, 125 μ M indomethacin, and 1 nM T3 (all from Sigma-Aldrich). Prewritten adipocytes were induced in standard medium supplemented with 500 μ M IBMX, 1 μ M dexamethasone, and 10 μ g/mL insulin. Cells were fully differentiated by day 6 after induction and transferred to a maintenance medium supplemented with 1 nM T3 and 20 nM insulin. Fully differentiated adipocytes were treated with 100 nM CL-316243, 50 μ M etomoxir, or 50 μ g/mL ranolazine (all from Sigma-Aldrich) for 24 h. Cells were cultured at 37 °C in a humidified incubator under a 5% CO₂ atmosphere. The medium was replaced every other day.

Cellular Respiration Analysis of Primary Brown Adipocytes. The cellular OCR of the primary brown adipocytes was determined using a Seahorse XF96 extracellular flux analyzer (Seahorse Bioscience). Differentiated adipocytes were plated at a density of 10,000 cells/well. The adipocytes were treated with 100 nM CL-316243 or 50 μ M etomoxir for 24 h. The baseline cellular OCR was measured in the untreated cells. The inhibitors of mitochondrial respiratory chain complexes, 1 μ M oligomycin (complex V inhibitor), 1 μ M carbonyl cyanide-4-(trifluoromethoxy)phenylhydrazone (FCCP; mitochondrial uncoupler), and 0.5 μ M rotenone/antimycin A (complex I/III inhibitor) were treated sequentially. The mitochondrial parameters including basal respiration, ATP

production, proton leak, and maximal respiration were calculated from the OCR before and after the addition of inhibitors. Basal respiration was derived by subtracting nonmitochondrial respiration from baseline cellular OCR. ATP production was determined by subtracting the oligomycin rate from baseline cellular OCR and proton leak by subtracting nonmitochondrial respiration from the oligomycin rate. The maximal respiration was calculated by subtracting nonmitochondrial respiration from the FCCP rate. Nonmitochondrial respiration was measured after addition of rotenone/antimycin A.

Statistical Analysis. The data are presented as mean \pm SEM. Statistical significance was determined using an unpaired 2-tailed Student's *t* test. *P* < 0.05 was considered to indicate statistically significant differences.

ACKNOWLEDGMENTS. This study was supported by grants from the National Research Foundation of Korea funded by the Ministry of Science, ICT, and Future Planning (NRF-2016R1A2B4014630, NRF-2014R1A4A1008625, and Korea Mouse Phenotyping Project 2013M3A9D5072550); a faculty research grant from Yonsei University College of Medicine for 2018 (6-2018-0168, to J.-Y.S.); and the Brain Korea 21 PLUS Project for Medical Science, Yonsei University.

1. A. J. Sadler, B. R. Williams, Interferon-inducible antiviral effectors. *Nat. Rev. Immunol.* **8**, 559–568 (2008).
2. A. G. Bowie, L. Unterholzner, Viral evasion and subversion of pattern-recognition receptor signalling. *Nat. Rev. Immunol.* **8**, 911–922 (2008).
3. L. B. Ivashkiv, L. T. Donlin, Regulation of type I interferon responses. *Nat. Rev. Immunol.* **14**, 36–49 (2014).
4. M. Uhlén *et al.*, Proteomics. Tissue-based map of the human proteome. *Science* **347**, 1260419 (2015).
5. A. I. Su *et al.*, A gene atlas of the mouse and human protein-encoding transcriptomes. *Proc. Natl. Acad. Sci. U.S.A.* **101**, 6062–6067 (2004).
6. C. Wu *et al.*, Gene set enrichment in eQTL data identifies novel annotations and pathway regulators. *PLoS Genet.* **4**, e1000070 (2008).
7. P. McClurg *et al.*, Genomewide association analysis in diverse inbred mice: Power and population structure. *Genetics* **176**, 675–683 (2007).
8. J. Y. Seo, R. Yaneva, P. Cresswell, Viperin: A multifunctional, interferon-inducible protein that regulates virus replication. *Cell Host Microbe* **10**, 534–539 (2011).
9. K. C. Chin, P. Cresswell, Viperin (vlg5), an IFN-inducible antiviral protein directly induced by human cytomegalovirus. *Proc. Natl. Acad. Sci. U.S.A.* **98**, 15125–15130 (2001).
10. X. Wang, E. R. Hinson, P. Cresswell, The interferon-inducible protein viperin inhibits influenza virus release by perturbing lipid rafts. *Cell Host Microbe* **2**, 96–105 (2007).
11. D. Jiang *et al.*, Identification of five interferon-induced cellular proteins that inhibit west Nile virus and dengue virus infections. *J. Virol.* **84**, 8332–8341 (2010).
12. M. A. Rivieccio *et al.*, TLR3 ligation activates an antiviral response in human fetal astrocytes: A role for viperin/vlg5. *J. Immunol.* **177**, 4735–4741 (2006).
13. T. Saitoh *et al.*, Antiviral protein Viperin promotes Toll-like receptor 7- and Toll-like receptor 9-mediated type I interferon production in plasmacytoid dendritic cells. *Immunity* **34**, 352–363 (2011).
14. L. Q. Qiu, P. Cresswell, K. C. Chin, Viperin is required for optimal Th2 responses and T-cell receptor-mediated activation of NF-kappaB and AP-1. *Blood* **113**, 3520–3529 (2009).
15. J. Y. Seo, R. Yaneva, E. R. Hinson, P. Cresswell, Human cytomegalovirus directly induces the antiviral protein viperin to enhance infectivity. *Science* **332**, 1093–1097 (2011).
16. J. Y. Seo, P. Cresswell, Viperin regulates cellular lipid metabolism during human cytomegalovirus infection. *PLoS Pathog.* **9**, e1003497 (2013).
17. E. R. Hinson, P. Cresswell, The N-terminal amphipathic alpha-helix of viperin mediates localization to the cytosolic face of the endoplasmic reticulum and inhibits protein secretion. *J. Biol. Chem.* **284**, 4705–4712 (2009).
18. E. D. Rosen, B. M. Spiegelman, Adipocytes as regulators of energy balance and glucose homeostasis. *Nature* **444**, 847–853 (2006).
19. K. A. Lo, L. Sun, Turning WAT into BAT: A review on regulators controlling the browning of white adipocytes. *Biosci. Rep.* **33**, e00065 (2013).
20. L. Sidossis, S. Kajimura, Brown and beige fat in humans: Thermogenic adipocytes that control energy and glucose homeostasis. *J. Clin. Invest.* **125**, 478–486 (2015).
21. K. Ikeda, P. Maretich, S. Kajimura, The common and distinct features of brown and beige adipocytes. *Trends Endocrinol. Metab.* **29**, 191–200 (2018).
22. M. Giralt, F. Villarroya, White, brown, beige/brn: Different adipose cells for different functions? *Endocrinology* **154**, 2992–3000 (2013).
23. A. Bartelt, J. Heeren, Adipose tissue browning and metabolic health. *Nat. Rev. Endocrinol.* **10**, 24–36 (2014).
24. A. Abdullahi, M. G. Jeschke, White adipose tissue browning: A double-edged sword. *Trends Endocrinol. Metab.* **27**, 542–552 (2016).
25. A. Pfeifer, L. S. Hoffmann, Brown, beige, and white: The new color code of fat and its pharmacological implications. *Annu. Rev. Pharmacol. Toxicol.* **55**, 207–227 (2015).
26. M. J. Hanssen *et al.*, Short-term cold acclimation improves insulin sensitivity in patients with type 2 diabetes mellitus. *Nat. Med.* **21**, 863–865 (2015).
27. P. Schrauwen, W. D. van Marken Lichtenbelt, Combating type 2 diabetes by turning up the heat. *Diabetologia* **59**, 2269–2279 (2016).
28. J. M. Ellis *et al.*, Adipose acyl-CoA synthetase-1 directs fatty acids toward beta-oxidation and is required for cold thermogenesis. *Cell Metab.* **12**, 53–64 (2010).
29. S. Ji *et al.*, Homozygous carnitine palmitoyltransferase 1b (muscle isoform) deficiency is lethal in the mouse. *Mol. Genet. Metab.* **93**, 314–322 (2008).
30. E. Gonzalez-Hurtado, J. Lee, J. Choi, M. J. Wolfgang, Fatty acid oxidation is required for active and quiescent brown adipose tissue maintenance and thermogenic programming. *Mol. Metab.* **7**, 45–56 (2018).
31. C. Guerra *et al.*, Abnormal nonshivering thermogenesis in mice with inherited defects of fatty acid oxidation. *J. Clin. Invest.* **102**, 1724–1731 (1998).
32. J. Lee, J. M. Ellis, M. J. Wolfgang, Adipose fatty acid oxidation is required for thermogenesis and potentiates oxidative stress-induced inflammation. *Cell Reports* **10**, 266–279 (2015).
33. P. Rajbhandari *et al.*, IL-10 signaling remodels adipose chromatin architecture to limit thermogenesis and energy expenditure. *Cell* **172**, 218–233.e17 (2018).
34. Y. Qiu *et al.*, Eosinophils and type 2 cytokine signaling in macrophages orchestrate development of functional beige fat. *Cell* **157**, 1292–1308 (2014).
35. R. R. Rao *et al.*, Meteorin-like is a hormone that regulates immune-adipose interactions to increase beige fat thermogenesis. *Cell* **157**, 1279–1291 (2014).
36. J. Eom *et al.*, Viperin deficiency promotes polarization of macrophages and secretion of M1 and M2 cytokines. *Immune Netw.* **18**, e32 (2018).
37. B. M. Spiegelman, J. S. Flier, Obesity and the regulation of energy balance. *Cell* **104**, 531–543 (2001).
38. L. E. Kuo *et al.*, Neuropeptide Y acts directly in the periphery on fat tissue and mediates stress-induced obesity and metabolic syndrome. *Nat. Med.* **13**, 803–811 (2007).
39. B. Cannon, J. Nedergaard, Brown adipose tissue: Function and physiological significance. *Physiol. Rev.* **84**, 277–359 (2004).
40. E. S. Bachman *et al.*, betaAR signaling required for diet-induced thermogenesis and obesity resistance. *Science* **297**, 843–845 (2002).
41. M. J. Betz, S. Enerbäck, Targeting thermogenesis in brown fat and muscle to treat obesity and metabolic disease. *Nat. Rev. Endocrinol.* **14**, 77–87 (2018).
42. D. Tupone, C. J. Madden, S. F. Morrison, Autonomic regulation of brown adipose tissue thermogenesis in health and disease: Potential clinical applications for altering BAT thermogenesis. *Front. Neurosci.* **8**, 14 (2014).
43. S. S. Evans, E. A. Repasky, D. T. Fisher, Fever and the thermal regulation of immunity: The immune system feels the heat. *Nat. Rev. Immunol.* **15**, 335–349 (2015).
44. J. K. Elmquist, T. E. Scammell, C. B. Saper, Mechanisms of CNS response to systemic immune challenge: The febrile response. *Trends Neurosci.* **20**, 565–570 (1997).
45. K. Nakamura, S. F. Morrison, Central efferent pathways for cold-defensive and febrile shivering. *J. Physiol.* **589**, 3641–3658 (2011).
46. B. Cannon, J. Nedergaard, Nonshivering thermogenesis and its adequate measurement in metabolic studies. *J. Exp. Biol.* **214**, 242–253 (2011).
47. E. Gospodarska, P. Nowialis, L. P. Kozak, Mitochondrial turnover: A phenotype distinguishing brown adipocytes from interscapular brown adipose tissue and white adipose tissue. *J. Biol. Chem.* **290**, 8243–8255 (2015).
48. Y. H. Tseng *et al.*, New role of bone morphogenetic protein 7 in brown adipogenesis and energy expenditure. *Nature* **454**, 1000–1004 (2008).